

# Entanglement estimation from Bell inequality violation

Karol Bartkiewicz,<sup>1,\*</sup> Bohdan Horst,<sup>2</sup> Karel Lemr,<sup>1</sup> and Adam Miranowicz<sup>2</sup>

<sup>1</sup>*RCPTM, Joint Laboratory of Optics of Palacký University and  
Institute of Physics of Academy of Sciences of the Czech Republic,  
17. listopadu 12, 772 07 Olomouc, Czech Republic*

<sup>2</sup>*Faculty of Physics, Adam Mickiewicz University, 61-614 Poznań, Poland*

It is well known that the violation of Bell's inequality in the form given by Clauser, Horne, Shimony, and Holt (CHSH) in two-qubit systems requires entanglement, but not vice versa, i.e., there are entangled states which do not violate the CHSH inequality. Here, we describe extremal states that have the maximal entanglement measured by the concurrence, negativity and relative entropy of entanglement for a given degree of the CHSH violation. We give an explicit expression for these states which happen to be the same for these three entanglement measures. For finding the extremal states we use a generalized method of Lagrange multipliers based on the Karush-Kuhn-Tucker conditions. The found states together with the states providing the lower bound on these entanglement measures for a given CHSH violation define the range of entanglement accessible for any two-qubit states that violate the CHSH inequality by the same amount. Furthermore, we describe an efficient experimental method to determine the degree of the CHSH violation for arbitrary two single-photon polarization qubits using six discrete measurement settings instead of nine settings required for obtaining a complete correlation matrix.

PACS numbers: 03.67.Mn, 03.65.Ud, 42.50.Dv

## 1. INTRODUCTION

Since the seminal paper of Einstein, Podolsky and Rosen [1], there has been much interest in two seemingly interrelated phenomena of quantum entanglement and nonlocality. Especially during the last three decades much theoretical and experimental work has been done in order to better understand these phenomena.

Quantum entanglement is nowadays relatively well understood [2] and defined as the inseparability of quantum states. This phenomenon was also a subject of intense studies having implications not only in physics but even in biology and philosophy.

Quantum nonlocality can be considered as a type of correlations between measurement outcomes, obtained in spatially and temporally separated laboratories, that cannot be explained by local hidden-variable theories. Bell-type inequalities [3, 4] are often used to address this nonlocality quantitatively [5]. For two qubits, Bell's inequalities are violated if their states are entangled. However, for higher-dimensional systems, there exist states exhibiting nonlocality without entanglement [6].

Moreover, as shown by Werner [7], there are entangled states that can still exhibit correlations which do not necessarily violate the Bell inequality in the form derived by Clauser, Horne, Shimony, and Holt (referred to as the CHSH inequality) [4]. Werner's states are defined for parameter  $p \in [0, 1]$  as [7]:

$$\hat{\rho}_W(p) = p|\Psi^-\rangle\langle\Psi^-| + \frac{1-p}{4} I \otimes I, \quad (1)$$

which is a mixture of the singlet state,  $|\Psi^-\rangle = (|01\rangle -$

$|10\rangle)/\sqrt{2}$ , and the maximally mixed state  $I \otimes I$ , where  $I$  is the identity operator. The Werner states violate the CHSH inequality iff  $1/\sqrt{2} < p \leq 1$ , while they are entangled iff  $1/3 < p \leq 1$ . Thus, for  $p \in (1/3, 1/\sqrt{2}]$ , the Werner states are entangled and satisfying the CHSH inequality [7]. These properties of the Werner states can be easily revealed by applying the Horodecki theorem [8].

Therefore, a natural question can be raised on how much entangled can be states without violating the CHSH inequality or, more general, for any fixed degree of the CHSH violation. The intuitive guess is that different measures of entanglement imply different answers for this question.

A degree of entanglement of two-qubit states can be described by various entanglement measures including [2]: (i) the relative entropy of entanglement (REE) [9], which is a quantum version of the Kullback-Leibler divergence; (ii) the Peres-Horodecki negativity [10], which is a measure of the entanglement cost under operations preserving the positivity of partial transpose (PPT) [11]; and (iii) the Wootters concurrence [12] being a measure of the entanglement of formation [13]. On the other hand, the Horodecki theorem [8] enables not only testing the CHSH inequality violation but also quantifying a degree of this violation for arbitrary two-qubit states. This degree is often referred to as a single-copy nonlocality measure [5].

In this paper we shall use the enlisted measures of entanglement to answer the question about the relation between the CHSH violation and entanglement quantitatively. In particular we find such states that have extreme entanglement for all the above-mentioned entanglement measures for a given degree of the CHSH violation. For the purpose of our optimization procedure we shall use the so-called Karush-Kuhn-Tucker (KKT) conditions in a generalized method of Lagrange multipliers,

\*Electronic address: bartkiewicz@jointlab.upol.cz

which provide powerful tools for solving such optimization problems [14]. We also use other tools for testing the optimality of the obtained states, namely the optimality conditions for the concurrence provided in Ref. [15] and Monte Carlo simulations.

We focus on the CHSH inequality, although there are stronger Bell inequalities as was shown for the Werner states by, e.g., Vertesi [16]. Note, however, that the CHSH inequalities even though simple (there is a variety of other Bell inequalities involving more measurement settings) are very powerful since the stronger inequality requires at least 465 settings on each side for the Vertesi inequality. The Werner states violate the Vertesi inequality for  $p > 0.7056$ , while the CHSH inequality is violated, as already mentioned for  $p > 1/\sqrt{2} \sim 0.7071$  only. There are other Bell inequalities that are not equivalent to the already mentioned ones. Notably, there is the Śliwa-Collins-Gisin inequality [17], i.e., the so-called  $I_{3322}$  inequality.

The paper is organized as follows. In Sec. 2 we review some basic definitions used throughout the paper. In the following Sec. 3 we provide the boundary states for a given value of the CHSH violation and analytic expressions for their entanglement in terms of the CHSH violation degree. The extremality conditions for the negativity and concurrence versus the CHSH violation are tested in Sec. 4 and Appendix A, respectively. Sec. 5 presents a description of an experimental proposal for measuring the CHSH violation degree using the same six settings regardless of the investigated two-qubit state. We conclude in Sec. 6.

## 2. PRELIMINARIES

Throughout this paper we study correlations in two-qubit systems described by density matrices  $\rho$ , which can be expressed in the standard Bloch representation as follows

$$\rho = \frac{1}{4}(I \otimes I + \vec{x} \cdot \vec{\sigma} \otimes I + I \otimes \vec{y} \cdot \vec{\sigma} + \sum_{n,m=1}^3 T_{nm} \sigma_n \otimes \sigma_m), \quad (2)$$

where the correlation matrix  $T_{ij} = \text{Tr}[\rho(\sigma_i \otimes \sigma_j)]$ , and vectors  $\vec{\sigma} = [\sigma_1, \sigma_2, \sigma_3]$ ,  $\vec{x}$  ( $\vec{y}$ ) with elements  $x_i = \text{Tr}[\rho(\sigma_i \otimes I)]$  ( $y_i = \text{Tr}[\rho(I \otimes \sigma_i)]$ ), are expressed in terms of the Pauli matrices. As discussed further in the text, this form of two-qubit density matrix is very convenient for investigating the CHSH violation.

### A. Measure of CHSH violation

In order to quantify the violation of the CHSH inequality, we use the Horodecki measure  $B$  [8] (in the form of Ref. [18]), which yields  $B = 0$  if the CHSH inequality is not violated and  $B = 1$  for the maximal violation. This

measure is defined as

$$B(\rho) \equiv \sqrt{\max[0, M(\rho) - 1]}, \quad (3)$$

where

$$M(\rho) = \max_{j < k} \{h_j + h_k\} \leq 2, \quad (4)$$

and  $h_j$  ( $j = 1, 2, 3$ ) are the eigenvalues of matrix  $U = T^T T$  constructed from the correlation matrix  $T$  and its transpose  $T^T$ . The CHSH inequality is violated for  $M(\rho) > 1$  [8]. In Sec. 5 we will describe how to measure the symmetric  $T^T T$  matrix directly providing the method of efficient estimation of  $B$ .

### B. Entanglement measures

In our considerations we apply three popular entanglement measures: the negativity, concurrence and REE.

The negativity is defined as [23]:

$$N(\rho) = \max[0, -2 \min \text{eig}(\rho^\Gamma)], \quad (5)$$

where  $\Gamma$  denotes partial transposition. The negativity is directly related to the logarithmic negativity, which has a direct physical meaning of the entanglement cost under the PPT operations [11, 24]. However, for convenience, we use the negativity instead.

The Wootters concurrence [12] is defined as

$$C(\rho) = \max\{0, 2 \max_j \lambda_j - \sum_j \lambda_j\}, \quad (6)$$

where  $\{\lambda_j^2\} = \text{eig}[\rho(\sigma_2 \otimes \sigma_2)\rho^*(\sigma_2 \otimes \sigma_2)]$ . This measure is a monotonic and convex function of the entanglement of formation [13]. Similarly as in the case of the negativity and logarithmic negativity, it is more convenient to operate with the concurrence instead of the entanglement of formation.

The REE is defined as

$$E_R(\rho) = \min_{\sigma \in \mathcal{D}} S(\rho||\sigma) = S(\rho||\sigma_0), \quad (7)$$

where  $S(\rho||\sigma) = \text{Tr}(\rho \log_2 \rho - \rho \log_2 \sigma)$  is the relative entropy to be minimized over a set  $\mathcal{D}$  of separable states  $\sigma$  [9, 19]. The REE is used to distinguish a density matrix  $\rho$  from the closest separable state (CSS)  $\sigma_0$ . For pure states, the REE reduces to the von Neumann entropy of one of the subsystems. However, the REE is not a true metric, because it is not symmetric and does not fulfill the triangle inequality. Analytical formula for  $\sigma_0$  (and thus for the REE) for a given general two-qubit state  $\rho$  is very unlikely to be found [20]. Nevertheless, there is a solution of the inverse problem [21]. Probably, the most efficient numerical method for calculating the REE was described in Ref. [22] and, thus, it is used here.

### 3. EXTREMAL ENTANGLEMENT FOR A GIVEN CHSH VIOLATION

For each of the three entanglement measures, listed in Sec. 2, we can ask about the states that are extremal, i.e., have maximal or minimal value of one entanglement measure for a given fixed value of another entanglement measure [20, 25–28] or the CHSH violation measure [15, 29, 30]. Similarly, we state a more specific question about the maximal entanglement for vanishing of any other fixed degree of the CHSH violation. In this section we show that for all the above-mentioned entanglement measures, the states of the highest (lowest) entanglement without violating the CHSH inequality are in fact the same states denoted as  $\rho_{\max}$  ( $\rho_{\min}$ ).

#### A. Optimal amplitude damped states

The amplitude-damped states can be defined by [30]:

$$\rho(\alpha, p) = p|\psi_\alpha\rangle\langle\psi_\alpha| + (1-p)|00\rangle\langle 00|, \quad (8)$$

where  $|\psi_\alpha\rangle = \sqrt{\alpha}|01\rangle + \sqrt{1-\alpha}|10\rangle$  with  $p, \alpha \in [0, 1]$ . As discussed in detail in Ref. [30], these states can be obtained by subjecting pure states  $|\psi_{\alpha'}\rangle$  to amplitude damping.

The amplitude-damped states, which provide the upper bound for the REE for a given value  $B$  of the CHSH violation, are the Bell-diagonal states as shown in Figs. 1(bottom) and 2. Moreover, as found in Ref. [30], the amplitude-damped states  $\rho(\alpha, p) \equiv \rho_{\max}(B_0)$ , having the maximal value of the REE,  $E_{R,\max}$ , for a given value  $B$ , are the following

$$p = \begin{cases} \frac{1}{4}(2 + \sqrt{2 + 2B^2}) & \text{if } B < B_0, \\ 1 & \text{if } B > B_0, \end{cases} \quad (9a)$$

$$1 \geq p \geq \frac{1}{4} \left( 2 + \sqrt{2 + 2B_0^2} \right) \text{ if } B = B_0, \quad (9b)$$

$$\alpha = \frac{1}{2p} \left( p - \sqrt{5p^2 - 4p - B^2} \right), \quad (9c)$$

where  $B_0 = 0.81686$ . For the negativity and concurrence for a given value of  $B$ , the states  $\rho_{\max}(B_0)$  are also optimal but for  $B_0 = 1$  [so  $p = \frac{1}{4}(2 + \sqrt{2 + 2B^2})$  for any  $B$ ] as shown in Sec. 4 and Appendix A, correspondingly. Thus, the maximal values of the entanglement measures for a given value of  $\xi = B^2 + 1$  is found as

$$N_{\max}(\xi) = \frac{\sqrt{2}}{4} \left( \xi + \sqrt{5\xi^2 - 2\sqrt{2}\xi + 2} \right) - \frac{1}{2}, \quad (10)$$

$$C_{\max}(\xi) = \frac{\sqrt{2}\xi^2 + 2\xi}{2\sqrt{\xi^2 + 2\sqrt{2}\xi + 2}}, \quad (11)$$

while  $E_{R,\max}(B)$  is given in Ref. [30].

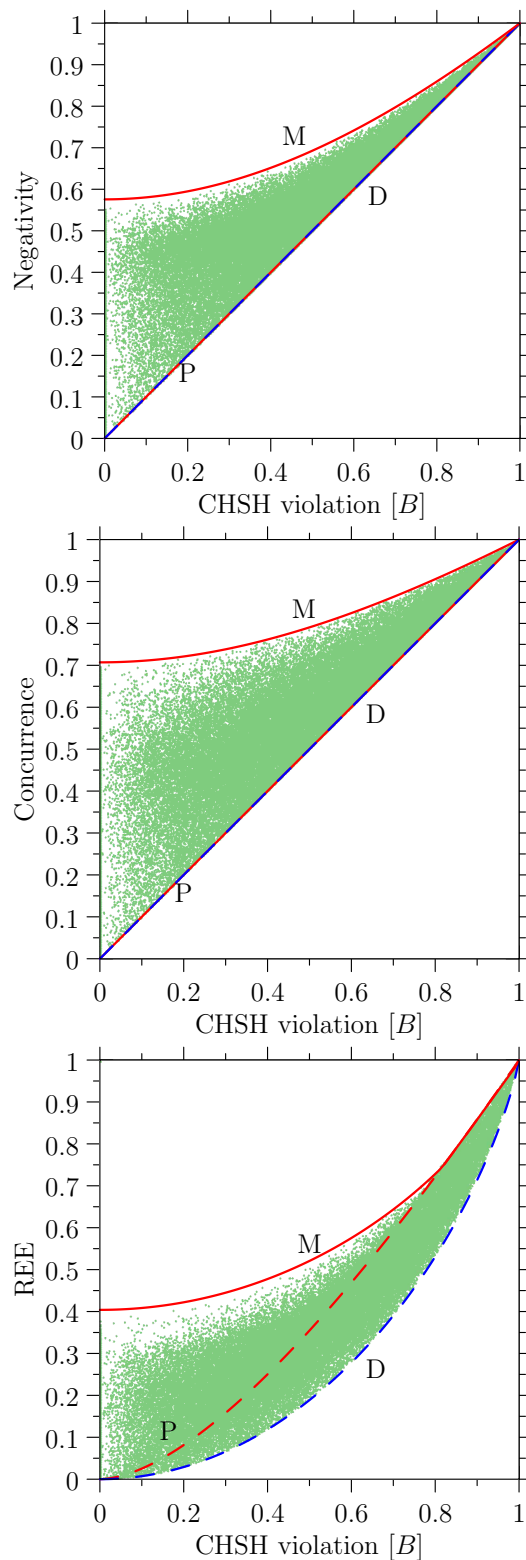


FIG. 1: (Color online) From the top: the negativity  $N$ , concurrence  $C$ , and relative entropy of entanglement  $E_R$  versus the CHSH violation  $B$  for  $10^6$  random two-qubit states. The extremal states are marked as P for pure, D for Bell-diagonal ( $\rho_{\min}$ ), and M for  $\rho_{\max}$  states. The maximal values of  $N_{\max}(B=0) = 0.57567$ ,  $C_{\max}(B=0) = 0.70711$ , and  $E_{R,\max}(B=0) = 0.404$  are reached for the M states  $\rho_{\max}$ .

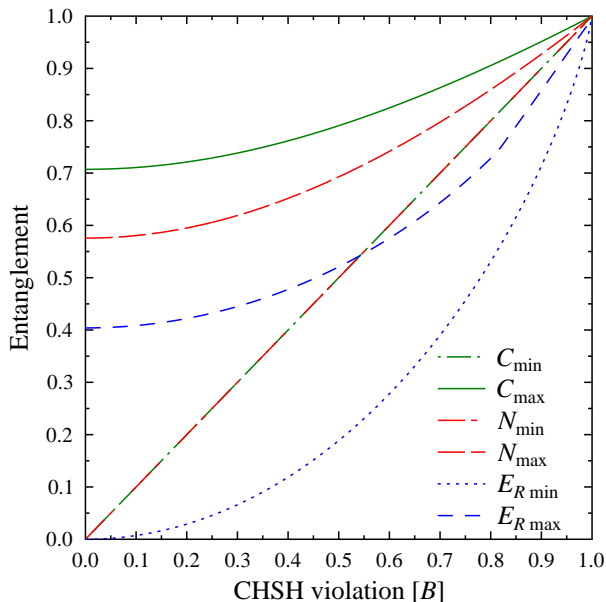


FIG. 2: (Color online) Comparison of the extremal values of the relative entropy of entanglement  $E_R$ , concurrence  $C$ , and negativity  $N$  as a function of the CHSH violation  $B$ .

### B. Optimal phase damped states

The lower bound on the three entanglement measures vs the CHSH violation  $B$  is achieved by the Bell-diagonal states as shown in Fig. 1. The reason why the Bell-diagonal states provide the lower bound for  $B$  given for a fixed function of the spectral properties of two-qubit density functions was explained in Ref. [15]. The Bell diagonal states can be produced by two-qubit pure states subjected to phase damping [30]. These states can be given in terms of the CHSH violation degree  $B$ :

$$\rho_{\min} = \frac{1}{2}[(1+B)|\beta_1\rangle\langle\beta_1| + (1-B)|\beta_2\rangle\langle\beta_2|], \quad (12)$$

where  $|\beta_1\rangle$  and  $|\beta_2\rangle$  denote two orthogonal Bell states. Note that the relation between the CHSH violation and entanglement for the Bell-diagonal states is very simple as given by

$$N_{\min}(B) = C_{\min}(B) = B, \quad (13a)$$

$$E_{R\min}(B) = 1 - h[(1+B)/2], \quad (13b)$$

where  $h(x) = -x \log_2 x - (1-x) \log_2(1-x)$  is the binary entropy.

## 4. EXTREMALITY CONDITIONS FOR NEGATIVITY FOR A GIVEN CHSH VIOLATION

Here, we show that the amplitude-damped states, given by Eq. (8), for the parameters:

$$p = \frac{1}{4} \left( 2 + \sqrt{2(B^2 + 1)} \right), \quad (14a)$$

$$\alpha = \frac{1}{2} \left( 1 - \sqrt{1 - \frac{4(B^2 + 1)^2}{(B^2 + 1 + \sqrt{2})^2}} \right), \quad (14b)$$

are likely to provide the upper bound of the negativity  $N$  for a given value  $B$  of the CHSH violation. For this purpose we apply a generalized method of Lagrange multipliers and test the KKT conditions [14].

Thus, let us consider the following Lagrange function

$$\mathcal{L} = B(\rho) + l \left[ \frac{N}{2} - \text{Tr}(\rho(|\psi\rangle\langle\psi|)^\Gamma) \right] \quad (15)$$

$$- \text{Tr}(X\rho) + \lambda(\text{Tr}\rho - 1), \quad (16)$$

where  $l$ ,  $X$ , and  $\lambda$  are Lagrange multipliers,  $(|\psi\rangle\langle\psi|)^\Gamma$  is the optimal state for  $\rho$  providing  $N(\rho) = -2\text{Tr}[(|\psi\rangle\langle\psi|)^\Gamma\rho]$ .

The Lagrange function is stationary if it remains unchanged after arbitrary small deviation of  $\rho \rightarrow \rho + \Delta$ , where  $\Delta$  is defined on the support space of  $\rho$ . Thus, our Lagrange function

$$\mathcal{L} \rightarrow \mathcal{L} + \text{Tr}[\Delta(\mathcal{B}_{\text{CHSH}} + l(|\psi\rangle\langle\psi|)^\Gamma - X + \lambda)] \quad (17)$$

should remain constant for small  $\Delta$ , i.e.,

$$\mathcal{B}_{\text{CHSH}} + l(|\psi\rangle\langle\psi|)^\Gamma - X + \lambda = 0, \quad (18a)$$

$$X \geq 0, \quad \text{Tr}(X\rho) = 0, \quad (18b)$$

where  $\mathcal{B}_{\text{CHSH}}$  is the operator satisfying  $B(\rho) = \text{Tr}(\rho\mathcal{B}_{\text{CHSH}})$ . Let us also note that  $X \geq 0$  is required only for the eigenvalues in the support space of  $\rho$ .

Moreover, it follows from Eq. (18a), after taking the mean value for  $\rho$ , that

$$\lambda = l \frac{N}{2} - B(\rho). \quad (19)$$

Thus, we can rewrite the KKT conditions as

$$X = \mathcal{B}_{\text{CHSH}} - B(\rho) + l \left( \frac{N(\rho)}{2} + (|\psi\rangle\langle\psi|)^\Gamma \right) \geq 0,$$

$$\text{Tr}(X\rho) = 0. \quad (20)$$

For the following rank-2 mixed states  $\rho = \lambda_1|e_1\rangle\langle e_1| + \lambda_2|e_2\rangle\langle e_2|$ , which we conjecture to be extremal on the basis of our numerical simulation, we can easily derive the following expressions that can be used to the  $l$  multiplier as

$$\langle e_1 | \mathcal{B}_{\text{CHSH}} | e_2 \rangle = -l \langle e_1 | (|\psi\rangle\langle\psi|)^\Gamma | e_2 \rangle, \quad (21a)$$

$$\langle e_1 | \mathcal{B}_{\text{CHSH}} | e_1 \rangle = -l \left( \frac{N(\rho)}{2} + \langle e_1 | (|\psi\rangle\langle\psi|)^\Gamma | e_1 \rangle \right) + B(\rho). \quad (21b)$$

By applying the KKT conditions we can check if a given state is optimal having its  $\mathcal{B}_{\text{CHSH}}$  and  $(|\psi\rangle\langle\psi|)^\Gamma$ . The CHSH operator for the amplitude-damped states reads as

$$\mathcal{B}_{\text{CHSH}} = \begin{cases} \eta_1 \left[ (1-2p)\sigma_3^{\otimes 2} + 2p\sqrt{(1-\alpha)\alpha}\sigma_1^{\otimes 2} - 1 \right] & \text{if } 4p^2(1-\alpha)\alpha - (1-2p)^2 < 0, \\ \eta_2 \left[ 2p\sqrt{(1-\alpha)\alpha}(\sigma_1^{\otimes 2} + \sigma_2^{\otimes 2}) - 1 \right] & \text{otherwise,} \end{cases} \quad (22)$$

where  $\eta_1 = 1/\sqrt{(1-2p)^2 + 4p^2\alpha(1-\alpha) - 1}$  and  $\eta_2 = 1/\sqrt{8p^2(1-\alpha)\alpha - 1}$ , whereas

$$|\psi\rangle = \mathcal{N} \left[ (\sqrt{q^2 + 4y^2} - 1)|00\rangle + 2y|11\rangle \right], \quad (23)$$

where  $y = p\sqrt{\alpha(1-\alpha)}$ ,  $q \equiv 1 - p$ , and  $\mathcal{N}$  is a normalization constant.

The above results allow us to conclude that the optimal amplitude-damped states  $\rho(\alpha, p)$ , which maximize the negativity  $N(\rho)$  for a given  $B(\rho)$ , are for the parameters  $p$  and  $\alpha$ , given by Eq. (14). These parameters are the same as those resulting in the maximum REE for a fixed  $B$  as given by Eq. (9) but with  $B_0 = 1$ .

Then the negativity for  $\rho_{\max}(1)$  can be readily found as given by Eq. (10), which reaches its maximum  $N_{\max} \approx 0.57567$  for  $B = 0$ . This result is confirmed by our Monte Carlo simulation shown in Fig. 1(top).

Similar reasoning confirms that the minimal negativity is reached by the  $\rho_{\min}$  states, given by Eq. (12).

## 5. PROPOSAL OF EFFICIENT MEASUREMENT OF CORRELATION MATRIX $T^T T$

Knowing the lower and upper bounds of the three entanglement measures for a given CHSH violation  $B$ , we are now able to deduce the range of entanglement of any two-qubit state for a fixed  $B$ . The expression for the CHSH violation  $B$  depends solely on the eigenvalues of the symmetric real matrix  $T^T T$ . Here, we present an efficient method for measuring this correlation matrix  $T^T T$ .

We can express the elements of this matrix using two copies  $\rho_1$  and  $\rho_2$  of the two-qubit state  $\rho$  as

$$(T^T T)_{m,n} = \text{Tr}[(\rho_{A_1 B_1} \otimes \rho_{A_2 B_2}) U_{A_1 A_2} \otimes (\sigma_m \otimes \sigma_n)_{B_1 B_2}], \quad (24)$$

where  $\rho_{A_1 B_1} \equiv \rho_1$  and  $\rho_{A_2 B_2} \equiv \rho_2$  for the subsystems  $A$  and  $B$ , whereas the operator  $U_{A_1 A_2} = (-4|\Psi^-\rangle\langle\Psi^-| + I)_{A_1 A_2}$  is given in terms of the singlet projection  $|\Psi^-\rangle\langle\Psi^-|$  onto the corresponding subsystems and the identity operation  $I$  (for a derivation see Appendix B). Since the  $3 \times 3$  matrix  $T^T T$  is symmetric,  $(T^T T)_{m,n} = (T^T T)_{n,m}$ , so it is completely defined by six real numbers, which can be directly measured for, e.g., single-photon polarization qubits. We choose, e.g.,  $|0\rangle$  ( $|1\rangle$ ) to represent a horizontally (vertically) polarized

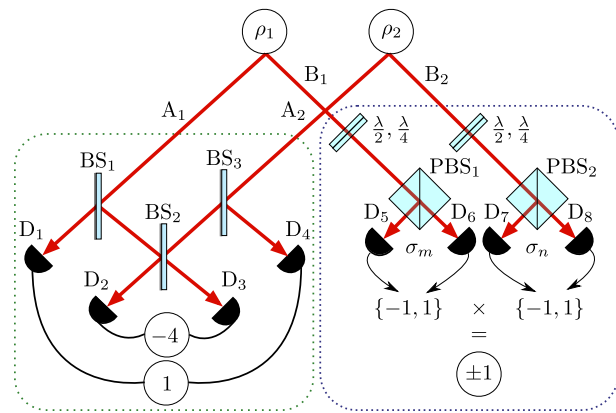


FIG. 3: (Color online) Setup implementing the measurement of  $(T^T T)_{m,n}$  using two sources (or a single photon source with routing and delaying every second pair of photons) of a two-qubit state ( $\rho_1$  and  $\rho_2$ ). The basic building blocks are as follows: the beam splitters (BSs), polarizing beam splitters (PBSs), quarter-wave plate ( $\lambda/4$ ) and half-wave plate ( $\lambda/2$ ), and standard detectors. The values of  $m, n = x, y, z$  are set by rotating the polarization by means of the wave plates, i.e., one  $\lambda/4$  and one  $\lambda/2$  plate, where  $\lambda$  is the wavelength. Circled  $-4$  (or  $\pm 1$ ) means that this value is assigned if the corresponding detectors (D) click. Since the investigated function of the correlation matrix  $T$  is symmetric we need only to measure it in six configurations, e.g.,  $(m, n) = (x, x), (x, y), (x, z), (y, y), (y, z), (z, z)$ . Due to probabilistic nature of the path taken by photons after the BS interaction, the setup gives conclusive result in half of the cases if  $\rho_1$  and  $\rho_2$  are supplied at the input.

photon. For such qubits,  $T^T T$  can be measured by the setup shown in Fig. 3. The left-hand side module of this setup, which consists of three 50:50 asymmetric beam splitters (BSs), performs the measurement of the  $U_{A_1 A_2}$  operator. The operation of this module was described in detail (considering imperfections including finite detection efficiency) in Ref. [31]. The possible outcomes for a single measurement instance  $a_k$  are  $a_k = -4, -1, 0, 1, 4$ , which are the product of the outcomes  $-4, 0, 1$  corresponding to a particular coincidence detection in the module:  $1$  – for a coincidence detection in the detectors  $D_1$  and  $D_4$ ,  $-4$  – for a coincidence detection in the detectors  $D_2$  and  $D_3$ , while  $0$  – if none of the two coincidences has been detected. Moreover, the right-hand side module of the setup in Fig. 3 measures the product  $\sigma_m \otimes \sigma_n$ . The outcomes  $-1, 1$  of this module occur for measuring the product of the Pauli matrices. The useful values of  $a_n \neq 0$  appear for the half of the cases when the states  $\rho_1$  and  $\rho_2$  are delivered and assuming perfect detectors. For realistic components (see the analysis in Ref. [31]), this setup would provide us with a good estimation of  $T^T T$  in a time period corresponding to switching between the six settings of  $\sigma_m \otimes \sigma_n$  instead of nine settings required for the full tomography of the  $T$  matrix. The obtained

expected values read

$$\langle \sigma_m \otimes \sigma_n \rangle = \frac{1}{K_0} \sum_{k=1}^K a_k, \quad (25)$$

where  $K_0 = \sum_{k=0}^K \delta_{|a_k|,1}$  and  $\delta_{|a_k|,1}$  is the Kronecker  $\delta$ . Note that the depicted measurement method is not limited to measuring  $B$  for any two-qubit state. It measures  $T^T T$ , which contains more information than the sum of the two largest eigenvalues used for calculating  $B$ .

### A. Proposal of experimental optimization

Here, we discuss an optimization of the setup to make it experimentally more feasible. Our implementation of the left-hand side module, depicted conceptually in Fig. 3, requires three balanced beam splitters and four detectors. From the experimentalist point of view, the larger is the number of components, the larger is the measurement error. For example, the splitting ratio of beam splitters is particularly sensitive to mount alignment and manufacturing precision. Furthermore all the detectors have to be calibrated to the same relative detection efficiency.

To reduce the number of required optical components, we propose a modified measurement setup depicted in Fig. 4. As the conceptual setup in Fig. 3 shows, there are two distinct measurement regimes in the module. The first regime is implemented by two-photon overlap on a balanced beam splitter projecting the state onto the singlet state. The corresponding coincidence rate is then multiplied by the factor of  $-4$ . The second regime is just a plain coincidence count (detectors  $D_1$  and  $D_4$ ). In the modified setup, we implement both these regimes using a single beam splitter. To switch between the regimes, we suggest a delay line to tune the temporal overlap between the interacting photons. The first measurement regime is obtained by setting the delay between the photons to zero, while the second regime is obtained when the delay is sufficiently larger than a single-photon coherence length. In the second regime, the two photons impinge on the beam splitter independently and they exit by different output ports in half of the cases only. For this reason, this number of coincidences has to be multiplied by 2 to implement the conceptual setup.

The benefits of the optimized setup are at least three-fold: (i) The number of beam splitters is reduced by a factor of three. (ii) The only one pair of detectors is used, so there is no need for the calibration within the module. The only calibration to be performed is the mutual calibration of the efficiencies of the detector pairs across the left and right hand side modules of the setup. (iii) Another minor benefit of the modified version of the setup is that it can be constructed using a standardized two-photon state characterization device [32] routinely used in other experiments. Note that since there is need for the singlet-state projection even in the original setup,

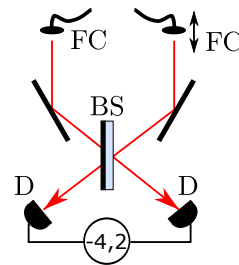


FIG. 4: (Color online) Experiment-friendly setup replacing the left-hand side measurement module in Fig. 3. BS – balanced beam splitter, FC – fiber coupler, D – detector. Motorized translation (marked by double arrow) is used to tune the temporal delay between the photons in order to switch between measurement regimes as explained in the text.

such delay line would be needed in order to stabilize the setup anyway. Therefore it does not impose any additional experimental requirements.

## 6. CONCLUSIONS

We have analyzed, as summarized in Fig. 2, the relation between the Horodecki measure of the CHSH inequality violation (or single-copy nonlocality) and three common entanglement measures: the negativity, concurrence and relative entropy of entanglement. We discovered optimal states that provide the upper bound on the entanglement measures for a given CHSH violation. We provided both numerical and analytic evidence by testing the KKT extremality conditions within a generalized Lagrange multiplier method in the case of the negativity for a given CHSH violation. We also checked that the found states satisfy the Verstraete-Wolf conditions [15] for the extremal concurrence for a given CHSH violation. Remarkably, the states are the same for all the investigated measures of entanglement, including the REE. We showed that the states providing the upper and lower bounds on the entanglement measures for a given value of the CHSH violation can be simply obtained by the amplitude and phase damping of pure states, respectively.

We also described a method how to efficiently measure the correlation matrix  $T^T T$ , and thus the degree of the CHSH violation, which together with the found bounds on the entanglement provide an easy and practical way of estimating entanglement for arbitrary two-qubit states with a fixed degree of the CHSH violation.

Finally, we mention one possible application of our results. Recently, the CHSH inequality has been proved extremely useful for verifying quantumness of a black box device (say, a claimed quantum computer) programmed to win the so-called CHSH game [33]. Thus, with the help of our results, by looking at the results of the CHSH game, we are able to estimate how much entanglement was used by the tested black box.

## Acknowledgments

This work was supported by the Polish National Science Centre under grant DEC-2011/03/B/ST2/01903. K. B. gratefully acknowledges the support by the Operational Program Research and Development for Innovations – European Regional Development Fund (project CZ.1.05/2.1.00/03.0058 and the Operational Program Education for Competitiveness - European Social Fund (project CZ.1.07/2.3.00/20.0017 of the Ministry of Education, Youth and Sports of the Czech Republic.

## Appendix A: States with extremal concurrence for a given CHSH violation

The conditions satisfied by the extremal amount of the CHSH violation for a fixed value of the concurrence were given by Verstraete and Wolf in Ref. [15]. Note that, for quantifying the CHSH violation, the authors of Ref. [15] used the following parameter  $\beta = 2\sqrt{B^2 + 1}$ . So, the CHSH inequality is satisfied for  $\beta \leq 2$ . Nevertheless, their results are valid also in our case since  $B$  is uniquely determined by  $\beta$ . In order to solve the optimization problem, the method of the Lorentz transformations on extended correlation matrix  $T$  was used in Ref. [15] to generate states of the constant concurrence. It was found that pure and Bell-diagonal states have the maximal concurrence for a given value  $B$  of the CHSH violation. While the lowest concurrence for a given  $B$  is achieved by, e.g., a mixture of a Bell state and a separable state orthogonal to it (the so-called Horodecki state). The summary of these results is shown in Fig. 1(middle).

The optimality of the states  $\rho_{\max}$ , given by Eqs. (8) and (14), for the whole range of  $B$  can be demonstrated using the optimality conditions given in Ref. [29]. This is straightforward since the matrix  $R_{m,n} = \langle \sigma_m \otimes \sigma_n \rangle$  (for  $m, n = 0, 1, 2, 3$ ), which was used for testing the optimality conditions in Ref. [15], has the same structure as  $\rho_{\max}$ . The relevant parameters as defined in Ref. [15] read as

$$a^{(\pm)} = -\frac{\sqrt{2}(\xi^2 - 2)}{4(\xi + \sqrt{2})} \pm \frac{\sqrt{2}}{4} \sqrt{\xi^2 + 2\sqrt{2}\xi + 2}, \quad (\text{A1a})$$

$$x = y = \frac{\sqrt{2}}{2}\xi, \quad z = -\frac{\sqrt{2}\xi + \xi^2}{\sqrt{2}\xi + 2}, \quad (\text{A1b})$$

where  $\xi^2 = B^2 + 1$ . These parameters satisfy the optimality conditions (in fact, they saturate the last two):

$$-1 \leq z \leq 1, \quad (\text{A2a})$$

$$(1+z)^2 - (a^{(+)} + a^{(-)})^2 \geq (x-y)^2, \quad (\text{A2b})$$

$$(1-z)^2 - (a^{(+)} - a^{(-)})^2 \geq (x+y)^2. \quad (\text{A2c})$$

Moreover, the concurrence for the amplitude-damped states is

$$C(\alpha, p) = 2p\sqrt{\alpha(1-\alpha)}, \quad (\text{A3})$$

so, in the case of the extremal states, it can be expressed by Eq. (11). Thus, the states  $\rho_{\max}$  belong to the class of states having the highest concurrence for a given degree  $B$  of the CHSH violation reaching the maximum  $C_{\max}(\xi = 1) \equiv C_{\max}(B = 0) = 1/\sqrt{2}$  as shown in Fig. 1(middle).

## Appendix B: Two-copy formula for correlation matrix $T^T T$

Here, we derive a two-copy formula for the correlation matrix  $T^T T$ , given by Eq. (24), which is useful for our experimental proposal.

In the following, we use the Einstein summation convention. Let us start from recalling that we can express  $T_{mn}$  as an expectation value of the Pauli matrices, i.e.,

$$T_{mn} = \text{Tr}[(\sigma_m \otimes \sigma_n)\rho], \quad (\text{B1})$$

hence

$$\begin{aligned} (T^T T)_{mn} &= T_{km} T_{kn} = \text{Tr}[(\sigma_k \otimes \sigma_m \otimes \sigma_k \otimes \sigma_n)(\rho \otimes \rho)] \\ &= \text{Tr}[(\sigma_k \otimes \sigma_k) \otimes (\sigma_m \otimes \sigma_n)(\rho \otimes \rho)'] \\ &= \text{Tr}\{[U_{A_1 A_2} \otimes (\sigma_m \otimes \sigma_n)_{B_1 B_2}]'(\rho \otimes \rho)\}, \end{aligned} \quad (\text{B2})$$

where  $(\rho \otimes \rho)' = S_{A_2 B_1}(\rho \otimes \rho)S_{A_2 B_1}$ ,  $U = \sigma_k \sigma_k = I - 4|\Psi^-\rangle\langle\Psi^-|$ , and  $|\Psi^-\rangle$  denotes the singlet state. The unitary transformation  $S_{A_2 B_1} = I \otimes S \otimes I$  swaps the modes  $A_2$  and  $B_1$ , which can be given in terms of the swap operator

$$S = \begin{pmatrix} 1 & 0 & 0 & 0 \\ 0 & 0 & 1 & 0 \\ 0 & 1 & 0 & 0 \\ 0 & 0 & 0 & 1 \end{pmatrix}. \quad (\text{B3})$$

Eq. (B2) finally results in Eq. (24).

- 
- [1] A. Einstein, and B. Podolsky, N. Rosen, Phys. Rev. **47**, 777 (1935).  
 [2] R. Horodecki, P. Horodecki, M. Horodecki, and K. Horodecki, Rev. Mod. Phys. **81**, 865 (2009).  
 [3] J. S. Bell, *Speakable and Unsayable in Quantum*

- Mechanics* (Cambridge University Press, Cambridge, United Kingdom, 2004).  
 [4] J. F. Clauser, M. A. Horne, A. Shimony, and R. A. Holt, Phys. Lett. A **23**, 880 (1969).  
 [5] N. Brunner, D. Cavalcanti, S. Pironio, V. Scarani, and

- S. Wehner, e-print arXiv:1303.2849.
- [6] C.H. Bennett, D.P. DiVincenzo, C.A. Fuchs, T. Mor, E. Rains, P.W. Shor, J.A. Smolin, and W.K. Wootters, *Phys. Rev. A* **59**, 1070 (1999).
- [7] R. F. Werner, *Phys. Rev. A* **40**, 4277 (1989).
- [8] R. Horodecki, P. Horodecki, and M. Horodecki, *Phys. Lett. A* **200**, 340 (1995); R. Horodecki, *Phys. Lett. A* **210**, 223 (1996).
- [9] V. Vedral, M. B. Plenio, M. A. Rippin, and P. L. Knight, *Phys. Rev. Lett.* **78**, 2275 (1997).
- [10] A. Peres, *Phys. Rev. Lett.* **77**, 1413 (1996); M. Horodecki, P. Horodecki, and R. Horodecki, *Phys. Lett. A* **223**, 1 (1996).
- [11] K. Audenaert, M. B. Plenio, and J. Eisert, *Phys. Rev. Lett.* **90**, 027901 (2003).
- [12] W. K. Wootters, *Phys. Rev. Lett.* **80**, 2245 (1998).
- [13] C. H. Bennett, D. P. DiVincenzo, J. A. Smolin, and W. K. Wootters, *Phys. Rev. A* **54**, 3824 (1996).
- [14] S. Boyd and L. Vandenberghe, *Convex Optimization*, (Cambridge University Press, Cambridge, 2004).
- [15] F. Verstraete and M. M. Wolf, *Phys. Rev. Lett.* **89** 170401 (2002).
- [16] T. Vertesi, *Phys. Rev. A* **78**, 032112 (2008).
- [17] C. Śliwa, *Phys. Lett. A* **317**, 165 (2003); D. Collins and N. Gisin, *J. Phys. A: Math. Gen.* **37**, 1775 (2004).
- [18] A. Miranowicz, *Phys. Lett. A* **327**, 272 (2004).
- [19] V. Vedral and M. B. Plenio, *Phys. Rev. A* **57**, 1619 (1998).
- [20] A. Miranowicz, S. Ishizaka, B. Horst, and A. Grudka, *Phys. Rev. A* **78**, 052308 (2008).
- [21] S. Ishizaka, *Phys. Rev. A* **67**, 060301(R) (2003); A. Miranowicz and S. Ishizaka, *Phys. Rev. A* **78**, 032310 (2008).
- [22] Y. Zinchenko, S. Friedland, and G. Gour, *Phys. Rev. A* **82**, 052336 (2010).
- [23] K. Życzkowski, P. Horodecki, A. Sanpera, and M. Lewenstein, *Phys. Rev. A* **58**, 883 (1998).
- [24] S. Ishizaka, *Phys. Rev. A* **69**, 020301(R) (2004).
- [25] F. Verstraete, K. M. R. Audenaert, J. Dehaene, and B. De Moor, *J. Phys. A* **34**, 10327 (2001).
- [26] T. C. Wei, K. Nemoto, P. M. Goldbart, P. G. Kwiat, W. J. Munro, and F. Verstraete, *Phys. Rev. A* **67**, 022110 (2003).
- [27] A. Miranowicz and A. Grudka, *Phys. Rev. A* **70**, 032326 (2004),
- [28] A. Miranowicz and A. Grudka, *J. Opt. B: Quantum Semi-class. Opt.* **6**, 542 (2004).
- [29] F. Verstraete, K. M. R. Audenaert, J. Dehaene, and B. De Moor, *J. Phys. A* **34**, 10327 (2001).
- [30] B. Horst, K. Bartkiewicz, and A. Miranowicz, *Phys. Rev. A* **87**, 042108 (2013).
- [31] K. Bartkiewicz, K. Lemr, A. Černoč, and J. Soubusta, *Phys. Rev. A* **87**, 062102 (2013).
- [32] E. Halenková, A. Černoč, K. Lemr, J. Soubusta, and S. Drusová, *Appl. Opt.* **51**, 474 (2012).
- [33] B. W. Reichardt, F. Unger, and U. Vazirani, *Nature (London)* **496**, 456 (2013).